Revista Virtual de Química

Article

http://dx.doi.org/10.21577/1984-6835.20250030

Investigation on the Interaction Between μ-oxo Trinuclear Ruthenium Complexes and DNA

Investigação Sobre a Interação entre os Complexos de Rutênio Trinucleares μ-oxo e o DNA

Sofia Nikolaou,[a] Otávio A. Chaves,*[b,c] Renan R. Bertoloni,[a] Bernardo A. Iglesias*[c]*

[a] Universidade de São Paulo, Faculdade de Filosofia, Ciências e Letras de Ribeirão Preto, Departamento de Química, Laboratório de Atividade Biológica e Química Supramolecular de Compostos de Coordenação (LABiQSC²), Zip Code 14040-901, Ribeirão Preto-SP, Brazil

[b] University of Coimbra, Coimbra Chemistry Centre – Institute of Molecular Sciences, Department of Chemistry, Zip Code 3004-535, Coimbra, Portugal

[c] Fundação Oswaldo Cruz (FIOCRUZ), Centro de Pesquisa, Inovação e Vigilância em COVID-19 e Emergências Sanitárias (CPIV), Laboratório de Imunofarmacologia, Zip Code 21040-361, Rio de Janeiro-RJ, Brazil

[d] Universidade Federal de Santa Maria, Laboratório de Bioinorgânica e Materiais Porfirínicos, Zip Code 97105-900, Santa Maria-RS, Brazil

***E-mail:** sofia@ffclrp.usp.br
otavioaugustochaves@gmail.com
bernardopgq@gmail.com

Submissão: 20 de Maio de 2025

Aceite: 30 de Junho de 2025

Publicado online: 7 de Julho de 2025

The μ-Oxo-trinuclear ruthenium acetates are promising metallodrug candidates and have been evaluated for their cytotoxicity against certain cancer cell lines, as well as for their anti-parasitic activity against *T. cruzi* and vasodilator profile. Therefore, the interaction between fish sperm deoxyribonucleic acid (fs-DNA) and the clusters $[Ru_3O(CH_3COO)_6(pic)_3]PF_6$ (**1**), $[Ru_3O(CH_3COO)_6(pic)_2(H_2O)]PF_6$ (**2**), $[Ru_3O(CH_3COO)_6(pic)_2(CO)]$ (**3**), $[Ru_3O(CH_3COO)_6(py)_2(H_2O)]PF_6$ (**4**), and $[Ru_3O(CH_3COO)_6(H_2O)_3]PF_6$ (**5**) (pic 3-picoline; py pyridine) was evaluated by steady-state fluorescence and viscosity measurements and molecular docking calculations. The capacity of compounds **1-5** to displace the probes ethidium bromide (EB), acridine orange (AO), 4',6-diamidino-2-phenylindole (DAPI), and methyl green (MG) was moderate to weak, with Stern-Volmer quenching constant (K_{sv}) values in the order of 10^3 to 10^4 M^{-1}. The highest constants consistently occurred for the DAPI probe, indicating that all compounds are minor groove binders, agreeing with the molecular docking trend, which also showed that van der Waals forces were mostly responsible for the interaction. Compounds **2**, **4**, and **5**, containing a labile water molecule in their structure, moderately changed the fs-DNA viscosity, signaling the possibility of coordinative binding. Finally, variation in hydrophobicity (presence or absence of a methyl group in the structure of the ligands) and charge did not lead to significant differences in the interaction profile.

Keywords: μ-oxo clusters; ruthenium; fs-DNA; metallodrugs; medicinal inorganic chemistry.

1. Introduction

Ruthenium compounds are extensively studied within coordination chemistry due to their application in a variety of areas, whether as catalysts, photosensitizers, or metallodrugs.[1–3] Among this last category, a class of ruthenium compounds that stands out are the μ-oxo trinuclear ruthenium acetate clusters, which have the general formula $[Ru_3O(CH_3COO)_6(L)_3]^n$ (L = H_2O, MeOH, DMSO, N-heterocycles, phosphines, CO or NO, with n = 0 or +1). For complexes with the same core structure (Figure 1), which are also common for other transition metals, the striking feature of the ruthenium case is the high electronic delocalization between the three metal ions and the μ-oxo bridge. The relative size of the Ru(III) and O^{2-} ions leads to effective orbital mixing, providing high electronic delocalization within the metallic unit, which is well described as an equilateral triangle. On the other hand, complexes with very π-acid ligands, such as carbon monoxide, tend to have lower electronic delocalization, since the coordination of this type of ligand requires the reduction of one of the three Ru ions to Ru(II) and usually promotes valence trapping due to the π-backbonding that takes place. Therefore, in carbonyl clusters in particular, there is a structural distortion to an isosceles triangle. These structural features generate distinct redox and electronic properties.[4,5]

In the last ten years, our research group has been working systematically on the biological properties of such compounds and has shown that they have anti-cancer, trypanocidal, and vasorelaxant activities.[5] When it comes to biotargets, our interest turned to their possible interaction with plasma proteins and deoxyribonucleic acid (DNA). Within the species investigated so far, we found that the interaction of this class of coordination complexes with human serum albumin (HSA) is strong, depending on structural features such as ancillary ligands and charge.[6–8] Additionally, the interaction with DNA was strong (DNA intercalator) for the trinuclear ruthenium complexes containing phenazine, e.g., $[Ru_3O(CH_3COO)_5(phenazine)(py)_2]PF_6$.[9]

Varying ancillary ligands (represented by L in the general molecular formula) can significantly change the electronic properties of these compounds,[5,6] as well as their ability to engage in weak interactions with other biomacromolecules. Our research aims to develop metallodrug candidates

based on μ-oxo trinuclear ruthenium acetate clusters. In this sense, DNA is an important biological target. Thus, the present study intends to conduct a preliminary evaluation of the interaction between a specially designed series of clusters (Figure 1) and fs-DNA. Ultimately, we will be able to conclude whether it is relevant to consider DNA as a target for our compounds. The series $[Ru_3O(CH_3COO)_6(pic)_3]PF_6$ (**1**), $[Ru_3O(CH_3COO)_6(pic)_2(H_2O)]PF_6$ (**2**), $[Ru_3O(CH_3COO)_6(pic)_2(CO)]$ (**3**), $[Ru_3O(CH_3COO)_6(py)_2(H_2O)]PF_6$ (**4**), and $[Ru_3O(CH_3COO)_6(H_2O)_3]PF_6$ (**5**) (pic 3-picoline; py = pyridine) was proposed to verify the influence of different ancillary ligands, namely water labile molecules; N-heterocyclic ligands (pyridine or 3-picoline) and CO. The presence of the carbonyl ligand imposes the reduction of one of the Ru(III) ions, making the respective complex neutral compared to the others, all of which have a +1 charge. Our strategy was to evaluate the ability of compounds **1-5** to displace the dyes ethidium bromide (EB), acridine orange (AO), 4',6-diamidino-2-phenylindole (DAPI), and methyl green (MG) from the fs-DNA structure, since EB and AO are known intercalators, while DAPI and MG are minor and major groove binders, respectively.[10–13] Finally, to offer a molecular-level explanation for the binding trend and interactive forces, molecular docking calculations were carried out.

2. Materials and Methods

All reagents employed in this work were analytical grade, purchased from Merck KGaA company (Darmstadt, Germany) and used as received. The μ-oxo trinuclear ruthenium acetate clusters **1**-**5** were synthesized by standard literature methods and were the same solids reported elsewhere.[14,15]

The competitive binding assays for fs-DNA by steady-state fluorescence emission analysis were performed as follow: solution of compounds **1**-**5** (0 to 100 μM) were gradually added to mixtures of fs-DNA (1.0 μM) and one of the following dyes: ethidium bromide (EB; general intercalator; 10 μM; λ_{exc} 531 nm, λ_{em} 550-850 nm), acridine orange (AO; A-T rich intercalator; 10 μM; λ_{exc} 492 nm, λ_{em} 500-800 nm), 4',6-diamidino-2- phenylindole (DAPI; minor groove binder; 10 μM; λ_{exc} 359 nm, λ_{em} 390-700 nm), and methyl green (MG; major groove binder; 10 μM; λ_{exc} 395 nm, λ_{em} 390-650 nm). All solutions were prepared in Tris-HCl buffer, pH 7.4, 0.1 M NaCl, with 5% DMSO. The fluorescence spectra were recorded on a Horiba Yvon Fluoromax plus spectrofluorimeter (em/exc slit 5.0 nm). The dye:fs-DNA adducts solutions were incubated for 3 minutes after the addition of compounds **1**-**5**. The Stern-Volmer quenching constant (K_{SV}) and the bimolecular quenching rate constant (k_q) for each compound were calculated according to the Stern-Volmer approximation (Equation (1)):

$$\frac{F_0}{F} = 1 + k_q \tau_0 [Q] = 1 + K_{SV} \quad (1)$$

where F_0 and F are the steady-state fluorescence emission intensities in the absence and presence of the quencher, respectively. The τ_0 and [Q] represent the lifetime of the dye:DNA adduct (EB 23.0 ns; AO 2.20 ns, DAPI 1.70 ns, and MG 2.80 ns)[10–13] and the concentration of the quencher, respectively. According to the equation, K_{SV} values are

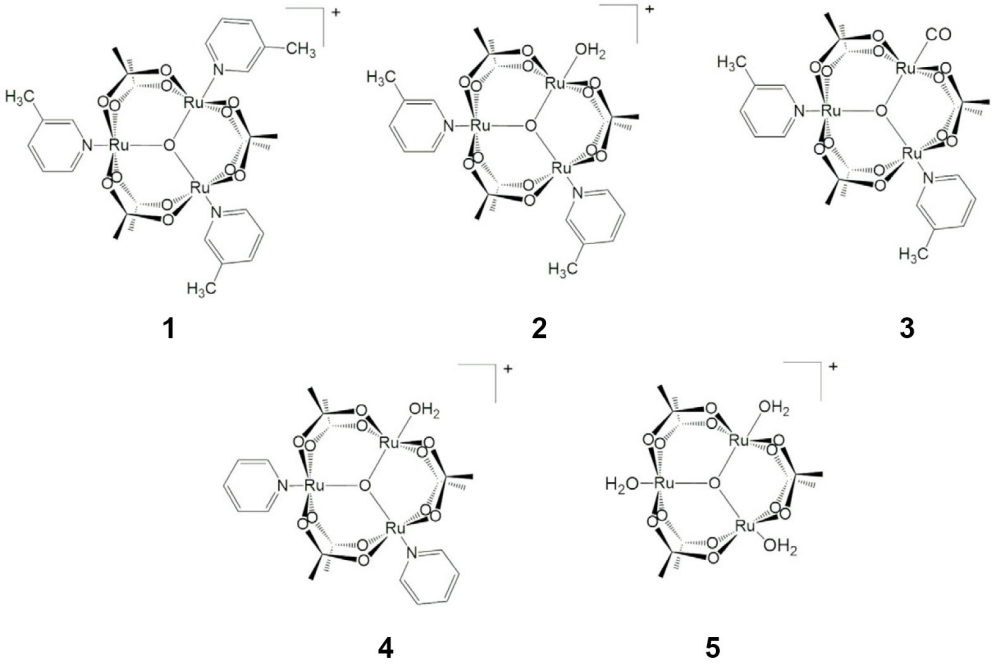

Figure 1. Chemical structure of μ-oxo trinuclear ruthenium acetate clusters studied in this work

calculated from the slope of a F_0/F vs [Q] plot (Stern-Volmer plot), and k_q is the ratio K_{SV}/τ_0.

Viscosity measurements were performed using an Ostwald viscometer immersed in a water bath at 298 K. The fs-DNA concentration was kept constant in all samples, and the concentration of compounds **1**-**5** varied from 0 to 50 μM in a Tris-HCl buffer solution (pH 7.4) with 5% DMSO. The flow time was measured at least in triplicate with a digital stopwatch, and the average value was calculated. Data are presented as a plot of $(\eta/\eta_0)^{1/3}$ vs [compound]/[fs-DNA], where η and η_0 are the specific viscosities of fs-DNA in the presence and absence of compounds **1**-**5**, respectively. The values of η and η_0 were calculated from the expression $(t - t_b)/t_b$, where t is the flow time for each sample and t_b is the buffer flow time. The relative viscosity of fs-DNA was calculated by η/η_0.[16]

The crystallographic structure of DNA was obtained from the Protein Data Bank (PDB code: 1BNA).[17] The chemical structure for complexes **1**-**5** was built and minimized in terms of energy by Density Functional Theory (DFT), available in the Spartan'18 software (Wavefunction, Inc., Irvine, CA, USA).[18] The molecular docking calculations for the ligands in the biomacromolecule model were performed with GOLD 2020.2 software (Cambridge Crystallographic Data Centre, Cambridge, CB2 1EZ, UK).[19] Hydrogen atoms were added to the DNA strands following tautomeric states and ionization data inferred by the software. The DNA structure presents two possible binding sites (major and minor grooves)[20] which were explored in the docking calculations via a 10 Å radius around each groove. ChemPLP was used as a scoring function, which is the default function of GOLD 2020.2 software that has the best correlation of *in silico* and *in vitro* data on the interaction between inorganic complexes and DNA.[21–23] The figures representing the docking poses for the largest docking score value were generated with the PyMOL Delano Scientific LLC program.[24]

3. Results and Discussion

The series of compounds shown in Figure 1 was designed to evaluate the following points: **Labile sites**: Compounds **2**, **4,** and **5**, which have labile water molecules in their peripheral positions, are the ones that could bind to the nucleobases of the DNA structure. Therefore, comparing their interaction profile with that of compounds **1** and **3** should allow us to evaluate this possibility. **The role of charge**: Charged complexes have the possibility of interacting electrostatically with the external phosphate skeleton of the DNA structure. By comparing neutral compound **3** with the other ones (all of them +1 charged species), we intend to assess the interaction of neutral and charged compounds of this class. **The role of methylation**: The literature discusses that the presence of methyl groups as substituents increases the hydrophobicity of a given chemical species.[25] This effect, in turn, could improve their interactions with biomolecules of interest. We therefore intend to probe the impact of methylation by comparing compounds **1-3** with compound **4**. To achieve this aim, we performed an investigation into DNA interaction using a competitive dye:fs-DNA study, viscosimetry, and molecular docking.

Figure 2 depicts the changes in the steady-state fluorescence emission spectra of dye:fs-DNA solutions upon successive additions of complex **4**, taken as a representative example (data for the other compounds and the Stern-Volmer plots are available in the Supplementary Information file, as Figures S1 to S40). The Stern-Volmer quenching constant (K_{SV}) values are shown in Table 1. Ethidium bromide (EB) and acridine orange (AO) were used as intercalator probes, while 4',6-diamidino-2-phenyl-indole (DAPI) and methyl green (MG) were used as minor and major groove markers, respectively.

In all cases, the steady-state fluorescence emission of the dye:fs-DNA adducts was partially quenched with the addition of the complexes, showing a competition between compounds **1-5** and the dyes for the fs-DNA interaction sites. Besides the decrease in fluorescence emission intensity, no red or blue shifts were observed (Figure 2 and Figures S1-S20), and the Ksv values range from 10^3 to 10^4 M^{-1} (Table 1, Figures 2 and S21-S40). The fact that the k_q are two to three orders of magnitude greater than the mean diffusion coefficient value for biomacromolecules (k_{diff} 7.40×10^9 $M^{-1}.s^{-1}$ at 298K, according to Smoluchowski-Stokes-Einstein theory),[26] suggests that the interaction between compounds **1-5** and fs-DNA occurs through a static mechanism. From a structural point of view of the inorganic complexes, none of them has in their structures large planar and conjugated fragments, although pyridine and 3-picoline have π–clouds available to engage in stacking interactions between the nucleobases of DNA. Therefore, these compounds are not expected to be good DNA intercalators. They are also charged (except compound **3**) and, especially in the case of compound **5**, tend to be more hydrophilic species. Accordingly, the highest K_{sv} values (in the order of 10^4 M^{-1}) and quenching capacities of over 50% (as measured by the Q parameter, Table 1) were observed for the DAPI probe, indicating that the clusters are good minor groove binders, not intercalators, agreeing with the molecular docking trend (Table 2). The only exception was compound **4** ($[Ru_3O(CH_3COO)_6(py)_2(H_2O)]PF_6$), which was able to quench 63% of the emission of the EB intercalation probe, indicating the possible intercalation of **4** with fs-DNA via minor groove approximation.

It is known that the viscosity of a DNA solution is dependent on its double helix arrangement in solution. When an intercalating molecule interacts with DNA, the double helix structure is disturbed, leading to an increase in DNA viscosity. This technique is considered superior to spectrophotometric titration because it is a direct measure of the compound:DNA interaction, assessing the presence or absence of the intercalation process.[27,28]

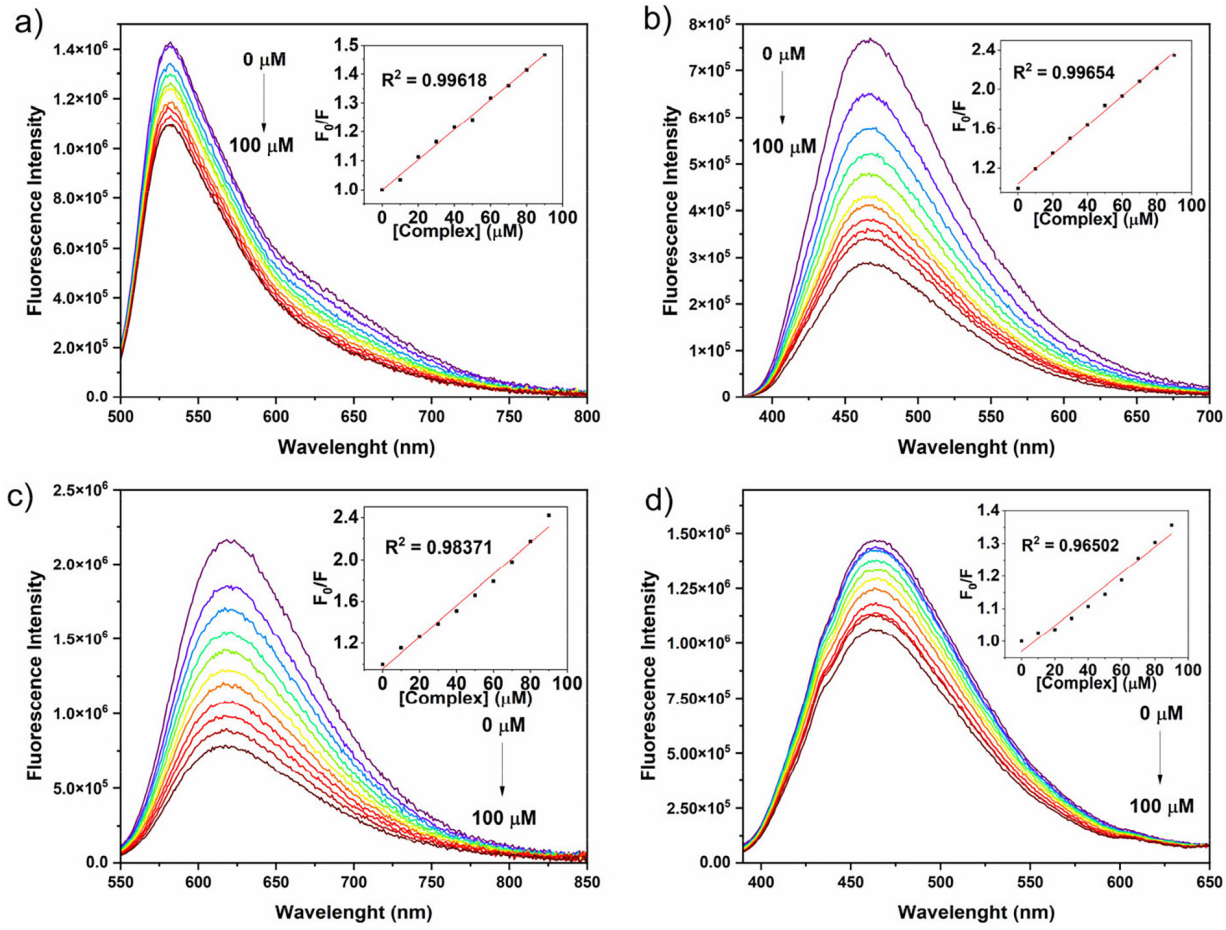

Figure 2. Steady-state fluorescence emission spectra for the interaction between fs-DNA and complex **4** in a DMSO (5%)/Tris-HCl pH 7.4 buffer mixture solution in the presence of (a) AO, (b) DAPI, (c) EB, and (d) MG dyes. Inset: Stern-Volmer plot for the interaction fs-DNA:dyes:compound **4** at the maximum fluorescence emission. [fs-DNA] 1 μm, [AO] [DAPI] [EB] [MG] 10 μm and [compound **4**] 0 to 100 μM

The results obtained for the interaction of compounds **1-5** are presented in Figure 3. For comparison purposes, the reference compounds EB, AO, and $[Ru(bpy)_3]^{2+}$ were also investigated.

Based on the variation in the viscosity of the fs-DNA:cluster adducts (Figure 3), none of the compounds proved to be good intercalators, in agreement with the steady-state fluorescence emission results. Compounds **1** and **3** showed profiles overlapping with that of the $[Ru(bpy)_3]Cl_2$ complex, a known standard for electrostatic interaction.[9] Surprisingly, the three species with water in their structures constitute an intermediate group, with an effect still much lower than that of typical intercalators such as EB and AO, but high enough to significantly modify the viscosity of the fs-DNA (Figure 3).

Compound **4** is the inorganic complex that had the most significant modification on the viscosity of fs-DNA, supporting the trend identified from the steady-state fluorescence data on dye-displacement assays. Despite their small size, both pyridine (present in compound **4**) and 3-picoline (present in compound **2**) ligands are aromatic organic molecules prone to interact with the nucleobases of fs-DNA. However, this interaction might be unfavorable in the case of the 3-picoline ligand, mainly due to the steric hindrance of the methyl group.[25] On the other hand, pyridine could be a feasible moiety for stacking interaction with DNA.

To aid the evaluation of the interaction mode between compounds **1-5** and DNA, *in silico* studies via molecular docking calculations were carried out. Table 2 shows the docking score values for DNA:compound into major and minor grooves. The docking score value (dimensionless) of each pose includes intramolecular tensions in the ligand and intermolecular interactions being considered as the negative value of the sum of energy terms involved in the macromolecule-ligand association; thus, the more positive the score suggest better the interactive profile.[19,21] Figure 4 depicts the best docking pose for the interaction between DNA (minor groove) and compound **1-5**, and Table 3 summarizes the main nucleobases, as well as their intermolecular forces and distances involved in the interaction process.

According to the *in silico* results all the compounds might interact with DNA structure, being accommodated mainly inside the minor groove (in about twenty to thirty punctuations higher than in the major groove, e.g. for

Table 1. Binding parameters for the competitive assays between fs-DNA:compounds and dyes (AO, DAPI, EB, and MG)

AO:fs-DNA			
Compound	**Q(%)[a]**	**K_{SV} (× 10^3 M^{-1})[b]**	**k_q (× 10^{11} M^{-1} s^{-1})[c]**
1	10.2	1.19	5.4
2	29.1	3.54	16.1
3	10.1	7.64	34.7
4	31.6	7.03	32.0
5	7.6	5.19	23.6
DAPI:fs-DNA			
Compound	**Q(%)[a]**	**K_{SV} (× 10^3 M^{-1})[b]**	**k_q (× 10^{11} M^{-1} s^{-1})[c]**
1	60.5	16.4	96.5
2	71.3	20.1	118.2
3	60.5	15.9	93.5
4	64.1	15.3	90.0
5	60.5	14.8	87.1
EB:fs-DNA			
Compound	Q(%)[a]	K_{SV} (× 10^3 M^{-1})[b]	k_q (× 10^{11} M^{-1} s^{-1})[e]
1	21.7	2.23	0.97
2	19.8	1.42	0.62
3	20.7	2.41	1.05
4	63.3	4.61	2.00
5	33.8	15.1	6.57
MG:fs-DNA			
Compound	**Q(%)[a]**	**K_{SV} (× 10^3 M^{-1})[b]**	**k_q (× 10^{11} M^{-1} s^{-1})[f]**
1	27.5	3.57	12.8
2	33.0	5.34	19.1
3	31.0	3.78	13.5
4	28.2	3.88	13.9
5	36.8	3.97	14.2

[a]Q(%) $(Em_{initial} - Em_{final})/(Em_{initial}) \times 100$; [b]Stern-Volmer quenching constant; [c]Bimolecular quenching rate constant (AO: τ_0 2.20 ns); [d]Bimolecular quenching rate constant (DAPI: τ_0 1.70 ns); [e]Bimolecular quenching rate constant (EB: τ_0 23.0 ns); [f]Bimolecular quenching rate constant (MG: τ_0 2.8 ns).

Table 2. Molecular docking score values (dimensionless) for the interaction between DNA and compounds **1-5** and dyes into the major and minor grooves of DNA

Compound	**Major Groove**	**Minor Groove**
1	20.1	41.9
2	16.2	38.8
3	17.0	39.5
4	18.3	43.1
5	10.1	28.2
AO[23]	68.1	50.2
DAPI[23]	------	81.5
EB[21]	65.3	36.7
MG[23]	28.3	------

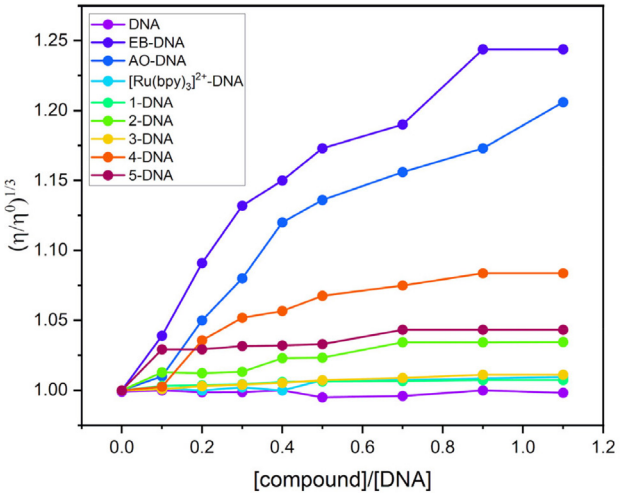

Figure 3. Effect of increasing concentration of compounds **1-5** on the relative viscosity of fs-DNA at 298 K

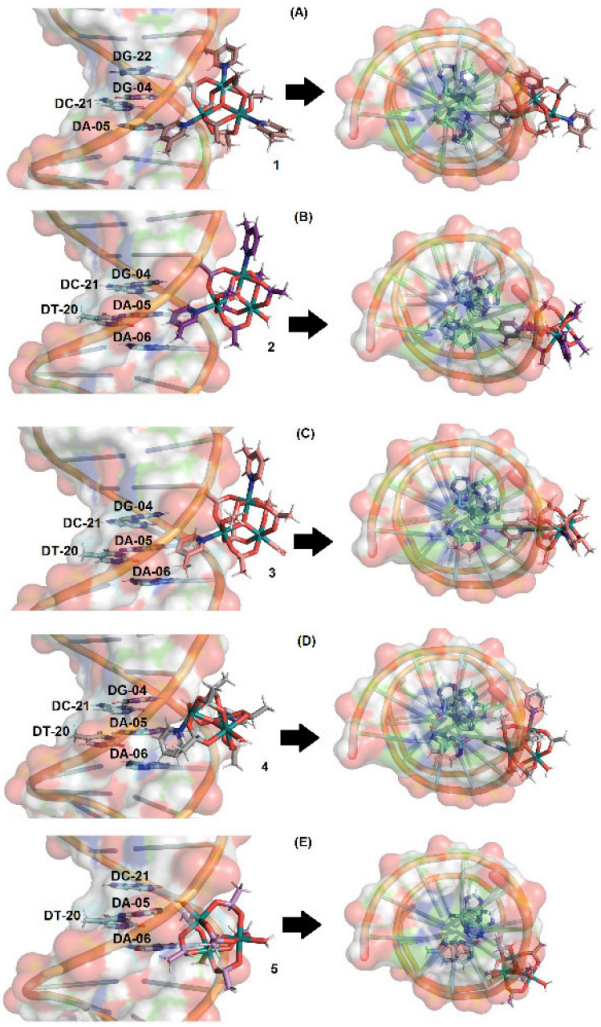

Figure 4. Best docking pose (ChemPLP function) for the interaction between (A) DNA:**1**, (B) DNA:**2**, (C) DNA:**3**, (D) DNA:**4**, and (E) DNA:**5** in the minor groove. Selected nitrogenated bases are in stick representation in cyan color, while **1**, **2**, **3**, **4**, and **5** are represented in brown, purple, beige, gray, and violet colors, respectively. Elements' color: hydrogen: white; oxygen: red; nitrogen: dark blue; and ruthenium: green

DNA:**2** is 16.2 and 38.8 dimensionless for major and minor grooves, respectively), agreeing with the experimental trend described in this work (dye-displacement assays in Table 1). The highest docking score values in the minor groove were obtained for the inorganic complex **4**, probably due to its capacity to be more buried into the DNA strands, as previously identified by the experimental trend on the capacity of **4** to quench 63% of the emission of the EB intercalation probe (Table 1). On the other hand, the lowest docking score value into the minor groove was obtained for the inorganic complex **5**, highlighting the importance of pyridine or 3-picoline moieties in the interactive profile with DNA. From literature, it has already been reported experimentally and *in silico* analysis that some Ru(II) complexes, e.g., $[Ru(bpy)_2Cl]^+$-porphyrins, $[Ru_2(bpy)_4(bip\text{-}phenol)]^{4+}$, and $[\{(bpy)_2Ru\}_2(4\text{-}azo)]^{4+}$ can interact with the minor groove of DNA.[29–31] Additionally,

Table 3. Molecular docking results for the interaction between DNA and compounds **1-5** in the minor groove

Compound	Nucleobase Residues	Interaction	Distance (Å)
1	DG-04	Van der Waals	2.80
	DA-05	Van der Waals	2.10
	DC-21	Van der Waals	2.90
	DG-22	Van der Waals	3.60
2	DG-04	Van der Waals	3.70
	DA-05	Van der Waals	3.70
	DA-06	Van der Waals	3.30
	DT-20	Van der Waals	2.90
	DC-21	Van der Waals	2.80
3	DG-04	Van der Waals	2.80
	DA-05	Van der Waals	2.10
	DA-06	Van der Waals	3.50
	DT-20	Van der Waals	3.10
	DC-21	Van der Waals	2.80
4	DG-04	Van der Waals	1.90
	DA-05	Van der Waals	1.80
	DA-06	Van der Waals	2.80
	DT-20	Van der Waals	3.00
	DC-21	Van der Waals	3.70
5	DA-05	Van der Waals	3.20
	DA-06	Van der Waals	3.50
	DT-20	Van der Waals	3.40
	DC-21	Van der Waals	3.00

molecular docking results suggested van der Waals forces (a type of weak electrostatic interaction) as the main intermolecular forces involved in the binding process, as an example, inside the minor groove of DNA strands, the chemical structure of the inorganic complex **1** can interact via van der Waals forces with four nucleobase residues: DG-04, DA-05, DC-21, and DG-22 within 2.80, 2.10, 2.90, and 3.60 Å, respectively, being supported by the experimental viscosity assays (Figure 3) described above.

Interestingly, the molecular docking results did not identify any hydrogen bonding contributions to the DNA:1-5 interaction (see Table 3), including for aquo compounds **2**, **4** and **5**. These observations provide an alternative explanation to intercalation for the release of EB into the solution, as evidenced by the quenching of 63% of its emission and a modest increase in DNA viscosity, both of which were caused by compound **4**. The main role of the coordinated water molecules may not be to facilitate weak interactions through hydrogen bonds; rather, they may be exchanged in the coordination sphere of the corresponding ruthenium ion through a coordinative interaction with a nitrogenous base residue, as suggested by the docking pose obtained for DNA:**5** (Figure 4E). Alternatively, they may create a different polarity environment to favor interaction with DNA driven by the hydrophobic moiety

of the inorganic complex, as suggested by the docking poses obtained for DNA:**2** and DNA:**4** (Figures 4B and 4D, respectively). Therefore, the double helix of the fs-DNA would be disturbed, resulting in a change in viscosity, as illustrated in Figure 3. In any case, further investigation is needed to fully assign the interactions of the aquo complexes **2**, **4**, and **5**.

Overall, considering the low variance of the experimental K_{sv} values in the presence of DAPI probe, the methylation of the ancillary ligands did not significantly change the intensity or the nature of their interaction with fs-DNA when comparing picoline to pyridine. The exception lies in the aquo compound **5** ($[Ru_3O(CH_3COO)_6(H_2O)_3]PF_6$), in which the absence of any N-heterocyclic ligand lowers the score. Finally, in our experimental conditions, the charge also did not imply any change in the type and intensity of interaction with the fs-DNA, since compound **3**, the only neutral species, did not show any deviation from the pattern of behavior observed for the other examples in the series.

4. Conclusions

In this work, we intended to evaluate the interaction of some representative examples of μ-oxo trinuclear ruthenium acetate clusters with fs-DNA. Our strategy was to verify it by molecular docking calculations, fs-DNA viscosity measurements, and the capacity of compounds **1-5** to displace the intercalation probes EB and AO, or the groove binder probes DAPI and MG (minor and major grooves, respectively). This series was designed to verify the influence of aspects such as ligand lability, complex charge, and hydrophobicity. We demonstrated that these compounds are weak interacting molecules, with Stern-Volmer quenching constant (K_{sv}) values in the order of 10^3 to 10^4 M^{-1}. All the compounds investigated in this work are minor groove binders, as probed by the highest K_{sv} values for the displacement of DAPI, corroborating the molecular docking trend. It was also shown that van der Waals forces are the main responsible for the interaction. In the case of compounds **2**, **4**, and **5**, which contain labile water molecules in their structure, the fs-DNA viscosity is moderately changed, suggesting the possibility of coordinative interactions occurring and consequent alteration in the double-helix conformation of fs-DNA. Variation in hydrophobicity, addressed by the presence or absence of a methyl group in the picoline and pyridine ligands, respectively, and variation in charge did not lead to differences in the observed interaction profile.

Supplementary Information

The following supporting information can be downloaded at https://rvq.sbq.org.br/, Figures S1 to S20: Steady-state fluorescence emission spectra for dyes: fs-DNA adducts in the presence and absence of variable concentrations of compounds 1-5; Figures S20 to S40: The Stern-Volmer plots for the corresponding fluorescence quenching data.

Acknowledgements

This research was funded by Fundação de Amparo à Pesquisa do Estado de São Paulo (FAPESP, grant numbers 2018/18060-3; 2022/03478-8; 2022/08085-4), Coordenação de Aperfeiçoamento de Pessoal de Nível Superior (CAPES, grant number 001), and Conselho Nacional do Desenvolvimento Científico e Tecnológico (CNPq, grant numbers 305761/2021-8). The Coimbra Chemistry Centre is supported by funding from the Fundação para a Ciência e a Tecnologia (FCT, the Portuguese agency for scientific research) through the projects UIDB/00313/2020 (https://doi.org/10.54499/UIDB/00313/2020, accessed on February 2025) and UIDP/00313/2020 (https://doi.org/10.54499/UIDP/00313/2020, accessed on February 2025). OAC acknowledges Programa de Pós-Graduação em Biologia Celular e Molecular from Oswaldo Cruz Foundation (Rio de Janeiro, Brazil) and CAPES for the grant PIPD (process SCBA 88887.082745/2024-00 with subproject 31010016).

Author Contributions

Conceptualization, S.N. and B.A.I.; methodology, S.N.; O.A.C.; R.R.B. and B.A.I.; software, O.A.C.; validation, S.N., O.A.C. and B.A.I.; formal analysis, S.N.; O.A.C.; R.R.B. and B.A.I.; investigation, S.N.; O.A.C.; R.R.B. and B.A.I.; resources, S.N. and B.A.I.; data curation, S.N. and R.R.B.; writing—original draft preparation, S.N. and R.R.B.; writing—review and editing, S.N.; O.A.C. and B.A.I.; visualization, S.N.; O.A.C.; R.R.B. and B.A.I.; supervision, S.N. and B.A.I.; project administration, S.N. and B.A.I.; funding acquisition, S.N.; O.A.C. and B.A.I..

Bibliographic References

1. Aksakal, N. E.; Kazan, H. H.; Eçik, E. T.; Yuksel, F.; A novel photosensitizer based on a ruthenium II phenanthroline bis(perylenediimide) dyad: synthesis, generation of singlet oxygen and *in vitro* photodynamic therapy. *New Journal of Chemistry* **2018**, *42*, 17538. [Crossref]
2. Jawiczuk, M.; Kuźmierkiewicz, N.; Nowacka, A. M.; Moreń, M.; Trzaskowski, B.; Mechanistic, Computational Study of Alkene-Diazene Heterofunctional Cross-Metathesis Catalyzed by Ruthenium Complexes. *Organometallics* **2023**, *42*, 146. [Crossref]
3. Öztürk, B. Ö.; Aklan, M.; Karabulut Şehitoğlu, S.; Dosage delivery of chiral ruthenium catalysts using non-ionic surfactants for asymmetric transfer hydrogenation reactions in aqueous media. *Reaction Chemistry & Engineering* **2023**, *8*, 424. [Crossref]

4. Toma, H.; Araki, K.; Alexiou, A.; Nikolaou, S.; Dovidauskas, S.; Monomeric and extended oxo-centered triruthenium clusters. *Coordination Chemistry Reviews* **2001**, *219–221*, 187. [Crossref]
5. Nikolaou, S.; do Nascimento, L. G. A.; Alexiou, A. D. P.; Oxo-centered trinuclear ruthenium acetates: Structure and applications. *Coordination Chemistry Reviews* **2023**, *494*, 215341. [Crossref].
6. da Silva, C. F. N.; Possato, B.; Franco, L. P.; Ramos, L. C. B.; Nikolaou, S.; The role of ancillary ligand substituents in the biological activity of triruthenium-NO complexes. *Journal of Inorganic Biochemistry* **2018**, *186*, 197. [Crossref].
7. Possato, B.; Chrispim, P. B. H.; Alves, J. Q.; Ramos, L. C. B.; Marques, E.; de Oliveira, A. C.; da Silva, R. S.; Formiga, A. L. B.; Nikolaou, S.; Anticancer activity and DNA interaction of ruthenium acetate clusters bearing azanaphthalene ancillary ligands. *Polyhedron* **2020**, *176*, 114261. [Crossref]
8. da Silva, C. F. N.; Ramos, L. C. B.; Rohrabaugh, T. N.; Vandevord, J. M.; da Silva, R. S.; Turro, C.; Nikolaou, S.; Exploring the structure of a ruthenium acetate cluster for biological purposes. *Inorganic Chemistry Communications* **2020**, *114*, 107810. [Crossref]
9. da Silva, C. F. N.; Chrispim, P. B. H.; Possato, B.; Portapilla, G. B.; Rohrabaugh, T. N.; Ramos, L. C. B.; Santana da Silva, R.; de Albuquerque, S.; Turro, C.; Nikolaou, S.; Anticancer and antitrypanosomal activities of trinuclear ruthenium compounds with orthometalated phenazine ligands. *Dalton Transactions* **2020**, *49*, 16440. [Crossref]
10. Estandarte, A. K.; Botchway, S.; Lynch, C.; Yusuf, M.; Robinson, I.; The use of DAPI fluorescence lifetime imaging for investigating chromatin condensation in human chromosomes. *Scientific Reports* **2016**, *6*, 31417. [Crossref]
11. Mayer, J. C. P.; Acunha, T. V.; Rodrigues, O. E. D.; Back, D. F.; Chaves, O. A.; Dornelles, L.; Iglesias, B. A.; Synthesis, spectroscopic characterization and DNA/HSA binding studies of (phenyl/naphthyl)ethenyl-substituted 1,3,4-oxadiazolyl-1,2,4-oxadiazoles. *New Journal of Chemistry* **2021**, *45*, 471. [Crossref]
12. Sayed, M.; Krishnamurthy, B.; Pal, H.; Unraveling multiple binding modes of acridine orange to DNA using a multispectroscopic approach. *Physical Chemistry Chemical Physics* **2016**, *18*, 24642. [Crossref]
13. Heller, D. P.; Greenstock, C. L.; Fluorescence lifetime analysis of DNA intercalated ethidium bromide and quenching by free dye. *Biophysical Chemistry* **1994**, *50*, 305. [Crossref]
14. Cacita, N.; Possato, B.; da Silva, C. F. N.; Paulo, M.; Formiga, A. L. B.; Bendhack, L. M.; Nikolaou, S.; Investigation of a novel trinuclear μ-oxo ruthenium complex as a potential nitric oxide releaser for biological purposes. *Inorganica Chimica Acta* **2015**, *429*, 114. [Crossref]
15. da Silva, A. B.; dos Santos, N. A. P.; Bertoloni, R. R.; Sampaio de Oliveira-Filho, A. G.; Nikolaou, S.; CO release by redox stimuli and HSA interaction: Planning new CORMs based on μ-oxo triruthenium carbonyl clusters. *Polyhedron*, 117589. [Crossref]
16. Rodrigues, B. M.; Victória, H. F. V.; Leite, G.; Krambrock, K.; Chaves, O. A.; de Oliveira, D. F.; Garcia, R. de Q.; De Boni, L.; Costa, L. A. S.; Iglesias, B. A.; Photophysical, photobiological, and biomolecule-binding properties of new tri-cationic meso-tri(2-thienyl)corroles with Pt(II) and Pd(II) polypyridyl derivatives. *Journal of Inorganic Biochemistry* **2023**, *242*, 112149. [Crossref]
17. Drew, H. R.; Wing, R. M.; Takano, T.; Broka, C.; Tanaka, S.; Itakura, K.; Dickerson, R. E.; Structure of a B-DNA dodecamer: conformation and dynamics. *Proceedings of the National Academy of Sciences* **1981**, *78*, 2179. [Crossref]
18. Shao, Y.; Molnar, L. F.; Jung, Y.; Kussmann, J.; Ochsenfeld, C.; Brown, S. T.; Gilbert, A. T. B.; Slipchenko, L. V.; Levchenko, S. V.; O'Neill, D. P.; DiStasio Jr, R. A.; Lochan, R. C.; Wang, T.; Beran, G. J. O.; Besley, N. A.; Herbert, J. M.; Yeh Lin, C.; Van Voorhis, T.; Hung Chien, S.; Sodt, A.; Steele, R. P.; Rassolov, V. A.; Maslen, P. E.; Korambath, P. P.; Adamson, R. D.; Austin, B.; Baker, J.; Byrd, E. F. C.; Dachsel, H.; Doerksen, R. J.; Dreuw, A.; Dunietz, B. D.; Dutoi, A. D.; Furlani, T. R.; Gwaltney, S. R.; Heyden, A.; Hirata, S.; Hsu, C.-P.; Kedziora, G.; Khalliulin, R. Z.; Klunzinger, P.; Lee, A. M.; Lee, M. S.; Liang, W.; Lotan, I.; Nair, N.; Peters, B.; Proynov, E. I.; Pieniazek, P. A.; Min Rhee, Y.; Ritchie, J.; Rosta, E.; David Sherrill, C.; Simmonett, A. C.; Subotnik, J. E.; Lee Woodcock III, H.; Zhang, W.; Bell, A. T.; Chakraborty, A. K.; Chipman, D. M.; Keil, F. J.; Warshel, A.; Hehre, W. J.; Schaefer III, H. F.; Kong, J.; Krylov, A. I.; Gill, P. M. W.; Head-Gordon, M.; Advances in methods and algorithms in a modern quantum chemistry program package. *Phys. Chem. Chem. Phys.* **2006**, *8*, 3172. [Crossref]
19. Jones, G.; Willett, P.; Glen, R. C.; Leach, A. R.; Taylor, R.; Development and validation of a genetic algorithm for flexible docking. *Journal of Molecular Biology* **1997**, *267*, 727. [Crossref]
20. Bessega, T.; Chaves, O. A.; Martins, F. M.; Acunha, T. V.; Back, D. F.; Iglesias, B. A.; de Oliveira, G. M.; Coordination of Zn(II), Pd(II) and Pt(II) with ligands derived from diformylpyridine and thiosemicarbazide: Synthesis, structural characterization, DNA/BSA binding properties and molecular docking analysis. *Inorganica Chimica Acta* **2019**, *496*, 119049. [Crossref]
21. Dozza, B.; da Rocha, V. N.; Köhler, M. H.; Piquini, P. C.; Chaves, O. A.; Iglesias, B. A.; The photophysical, photobiological, and light-up calf-thymus-DNA sensor activity of Pd(II) and Pt(II) polypyridyl derivatives coordinated to vinyl-pyridyl corroles. *Journal of Molecular Structure* **2025**, *1321*, 140056. [Crossref]
22. Iglesias, B. A.; Peranzoni, N. P.; Faria, S. I.; Trentin, L. B.; Schuch, A. P.; Chaves, O. A.; Bertoloni, R. R.; Nikolaou, S.; de Oliveira, K. T.; DNA-Interactive and Damage Study with meso-Tetra(2-thienyl)porphyrins Coordinated with Polypyridyl Pd(II) and Pt(II) Complexes. *Molecules* **2023**, *28*, 5217. [Crossref]
23. Trentin, L. B.; Viana, A. R.; Iwersen, S.; Iglesias, B. A.; Chaves, O. A.; Schuch, A. P.; Light exposure of tetra-cationic porphyrins containing peripheral Pd-bipyridyl complexes and the induced effects on purified DNA molecule, fibroblast and melanoma cell lines. *Photochemistry and Photobiology* **2025**, *101*, 565. [Crossref]
24. Yuan, S.; Chan, H. C. S.; Hu, Z.; Using PyMOL as a platform for computational drug design. *WIREs Computational Molecular Science* **2017**, *7*, e1298. [Crossref]

25. Barreiro, E. J.; Kümmerle, A. E.; Fraga, C. A. M.; The Methylation Effect in Medicinal Chemistry. *Chemical Reviews* **2011**, *111*, 5215. [Crossref]
26. Montalti, M.; Credi, A.; Prodi, L.; Gandolfi, M. T.; *Handbook of Photochemistry*, 3rda. ed, CRC Press: Boca Raton, FL, USA, 2006.
27. Satyanarayana, S.; Dabrowiak, J. C.; Chaires, J. B.; Tris(phenanthroline)ruthenium(II) enantiomer interactions with DNA: Mode and specificity of binding. *Biochemistry* **1993**, *32*, 2573. [Crossref]
28. Sun, Y.; Lutterman, D. A.; Turro, C.; Role of Electronic Structure on DNA Light-Switch Behavior of Ru(II) Intercalators. *Inorganic Chemistry* **2008**, *47*, 6427. [Crossref]
29. Oliveira, V. A.; Terenzi, H.; Menezes, L. B.; Chaves, O. A.; Iglesias, B. A.; Evaluation of DNA-binding and DNA-photocleavage ability of tetra-cationic porphyrins containing peripheral $[Ru(bpy)_2Cl]^+$ complexes: Insights for photodynamic therapy agents. *Journal of Photochemistry and Photobiology B: Biology* **2020**, *211*, 111991. [Crossref]
30. Gonzalez, V.; Wilson, T.; Kurihara, I.; Imai, A.; Thomas, J. A.; Otsuki, J.; A dinuclear ruthenium(II) complex that functions as a label-free colorimetric sensor for DNA. *Chemical Communications* **2008**, 1868. [Crossref]
31. Mi, Y.-X.; Wang, S.; Xu, X.-X.; Zhao, H.-Q.; Zheng, Z.-B.; Zhao, X.-L.; A promising DNA groove binder and photocleaver based on a dinuclear ruthenium(II) complex. *Journal of the Chilean Chemical Society* **2019**, *64*, 4392. [Crossref]